

Wind-Tunnel Technique for Determining Stability Derivatives from Cable-Mounted Models

Robert M. Bennett* and Moses G. Farmer*
NASA Langley Research Center, Hampton, Va.
and

Richard L. Mohr† and W. Earl Hall Jr.‡
Systems Control, Inc. (Vt), Palo Alto, Calif.

System identification techniques in common use for extracting stability derivatives from flight test data have been adapted for application to data obtained from aeroelastically scaled flutter models flown in a wind tunnel on a cable-mount system. The concept has been applied with reasonable success to data from rigid models of a space shuttle orbiter and a fighter tested in the NASA Langley transonic dynamics tunnel. Further application of this technique should permit extraction of derivatives that include scaled flexibility effects, thereby obtaining additional information from the testing of expensive flutter models.

Nomenclature

b	= reference span, m
C_l	= rolling-moment coefficient, $\frac{\text{rolling moment}}{q_\infty S b}$
C_{l_p}	$= \frac{\partial C_l}{\partial (pb/2V)}$
C_{l_r}	$= \frac{\partial C_l}{\partial (rb/2V)}$
C_{l_β}	$= \partial C_l / \partial \beta$
C_n	= yawing-moment coefficient, $\frac{\text{yawing moment}}{q_\infty S b}$
C_{n_p}	$= \frac{\partial C_n}{\partial (pb/2V)}$
C_{n_r}	$= \frac{\partial C_n}{\partial (rb/2V)}$
C_{n_β}	$= \partial C_n / \partial \beta$
C_m	= pitching-moment coefficient, $\frac{\text{pitching moment}}{q_\infty S \bar{c}}$
C_{m_q}	$= \frac{\partial C_m}{\partial (\dot{q}\bar{c}/2V)}$
C_{m_α}	$= \partial C_m / \partial \alpha$
$C_{m_{\dot{\alpha}}}$	$= \frac{\partial C_m}{\partial (\dot{\alpha}\bar{c}/2V)}$
$C_{m_q} + C_{m_{\dot{\alpha}}}$	= damping in pitch parameter, 1/rad
C_Y	= side-force coefficient, $Y\text{-force}/q_\infty S$

C_{Y_p}	$= \frac{\partial C_Y}{\partial (pb/2V)}$
C_{Y_r}	$= \frac{\partial C_Y}{\partial (rb/2V)}$
C_{Y_β}	$= \partial C_Y / \partial \beta$
C_Z	= Z-force coefficient, $Z\text{-force}/q_\infty S$
C_{Z_α}	$= \partial C_Z / \partial \alpha$
\bar{c}	= reference chord, m
p, q, r	= angular velocities of model about X, Y, and Z axis, respectively, rad/s
q_∞	= freestream dynamic pressure, Pa
S	= reference area, m ²
V	= freestream velocity, m/s
α	= angle of attack, rad
β	= angle of sideslip, rad
η	= real part of characteristic root (damping), 1/s
ω	= imaginary part of characteristic root (frequency), 1/s
$(\dot{})$	= d/dt

The x-y-z body axes form a right-hand system with the positive x, y, and z directions pointing forward, to the right, and down, respectively.

Introduction

FOR several years transonic flutter and gust response tests of complete aircraft models have been performed in the NASA Langley transonic dynamics tunnel by "flying" the models on a cable mounting system.^{1,2} The models are both dynamically and elastically scaled, are extensively instrumented, and are expensive to build, calibrate, and test. Although some aileron effectiveness tests have been made with this system in the past,^{3,4} it was recognized that there was a potential for obtaining valuable stability derivative data from it. Since the restraint of the mount is soft, the stability of the model on the cable-mount system is closely related to free flight stability characteristics. In addition, the important effects of aeroelastic deformations on the derivatives would be included as the models are elastically scaled. Sting mounted flutter models have also been used in the past for the study of flexibility effects on stability derivatives.^{5,6} Modern system identification techniques have been developed to the extent that they are a tool for nearly routine use for extracting stability derivatives from flight test data.⁷⁻¹⁰ Application of these system identification techniques would thus appear to be

Presented as Paper 77-1128 at the AIAA 4th Atmospheric Flight Mechanics Conference, Hollywood, Fla., Aug. 8-10, 1977; submitted Sept. 29, 1977; revision received Jan. 30, 1978. Copyright © American Institute of Aeronautics and Astronautics, Inc., 1977. All rights reserved.

Index categories: Handling Qualities, Stability and Control; Aerodynamics; Testing, Flight and Control.

*Aerospace Engineer, Aeroelasticity Branch, Structures and Dynamics Division. Member AIAA.

†Research Engineer. Member AIAA.

‡Director of System Identification and Control Division. Associate Fellow AIAA.

a promising approach for the cable-mounted models also. This paper describes an investigation to evaluate the feasibility of extracting stability derivatives from cable-mounted models using a maximum likelihood method of system identification. The development of this technique was a joint effort between NASA Langley Aeroelasticity Branch and Systems Control, Inc. (Vt). The tests, instrumentation and data collection were performed by NASA Langley. The adaptation of the maximum likelihood method, computer program development, and data reduction were performed by Systems Control under NASA contract.

The elements of system identification are 1) the mathematical model, 2) the method for controlled excitation, 3) the instrumentation and data collection, and 4) the identification algorithm. Each of these elements is examined, and required refinements or adaptations from previous procedures are described. In addition, refinements to the cable mounting system were made which included an active feedback control system to permit the testing of unstable models. An overview of the development of these items is described in this paper.

The technique is applied to data from rigid models of an F-14 fighter aircraft and a space shuttle orbiter tested in the NASA Langley transonic dynamics tunnel. The results of applying this technique to a few selected test points are presented. Both longitudinal and lateral cases for low angles of attack are considered. A more detailed presentation of these results is given in Ref. 11.

Description of the Parameter Identification Technique and Tests

The elements of the identification technique interact strongly with each other and form an integrated system. For example, the cable-mount system contains elements of the excitation and instrumentation systems which, in turn, affect the test technique. The cable-mount system and its associated instrumentation are described first, and then the overall instrumentation, models and tests, and identification procedure.

Cable-Mount System

The cable-mount system used in these tests is a refinement of a system that has been used extensively for flutter tests in the NASA Langley transonic dynamics tunnel. A schematic of the mount system is shown in Fig. 1. It consists of two cable loops with their ends attached to the model with pin joints. One loop extends upstream and passes over pulleys on the walls of the tunnel and the other loop extends downstream and also over pulleys on the walls. Either or both loops can be vertical or horizontal. The loops are kept under a tension that can be remotely adjusted. A spring is included in the rear loop to minimize changes in stiffness as the model is displaced. Some versions of the mount have the pulleys in the model and the ends fixed to the wall, but the effects of the mount are essentially the same in both cases. Although the schematic of Fig. 1 shows the entire loops in the airstream, the center portions are actually routed around the test section for these tests.

The models tested during this investigation are shown on the cable mount in Fig. 2. The F-14 model is shown suspended by a removable spring and the shuttle model is shown suspended by an X-shaped cable snubber system which is removed for the present tests. For the F-14 model, the cable mount consists of a horizontal forward loop and vertical rear loop, whereas for the shuttle model, the mount consists of a vertical forward loop and horizontal rear cable loop.

In effect, the cable system is somewhat analogous to a spring mounting system for a model. Linear and rotational stiffnesses and elastic axis positions are determined by the tension level and geometric arrangement of the cables. Limited freedom in all directions, except for the fore and aft direction, is normally permitted. The effective rotational

spring constants are generally soft in comparison with the aerodynamic springs, but the effects of the springs lead to additional translational modes of motion vertically (plunge) and sideward, and sometimes in rolling rotation. The fore and aft limitation of course implies that phugoid-like motions which involve large fore and aft motions are suppressed. Within the framework of linearized theory the lateral and longitudinal effects of the mount are decoupled. As the flow velocity is varied, the models are kept in the center of the tunnel by manual remote operation of the aerodynamic controls of the model.

The stability of a model on the cable-mount system is dependent on the tension level in the cable loops, the geometry of the mount, and the basic aerodynamic stability of the model. Considerable work has been done in analyzing and developing a mathematical model and associated computer program for this system.^{1,2,12} As there are practical limits on the tension and geometry of the cable mount, stability over a large range of dynamic pressures and Mach numbers may be difficult to achieve. Furthermore, with recent aircraft con-

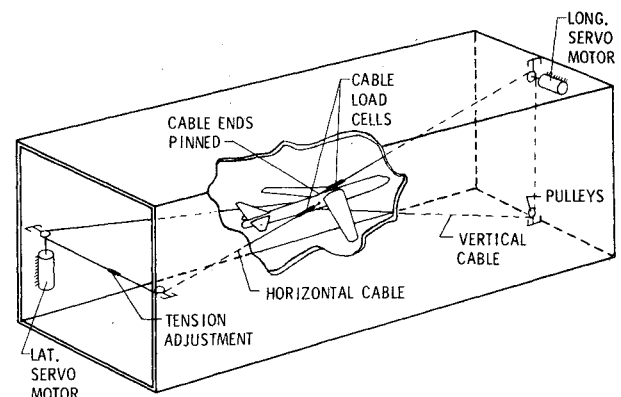
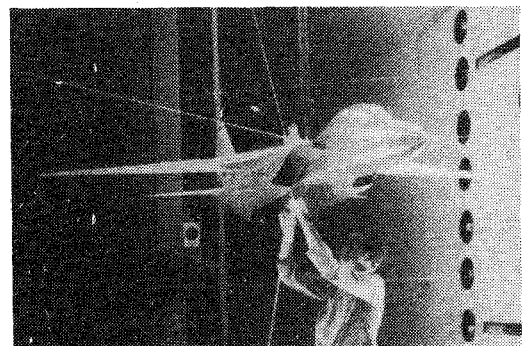
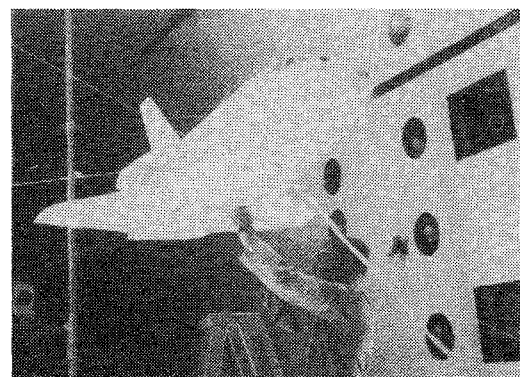


Fig. 1 Schematic of active two-cable mounting system.



a) F-14 model



b) Shuttle orbiter model

Fig. 2 Photographs of models mounted in the Langley transonic dynamics tunnel.

figurations there is a need to test models that have statically unstable aerodynamic characteristics. The two-cable system has been modified from the usual passive mounting system to an "active" system by placing a servo motor in each cable loop, which permits feedback operation for stability augmentation. The active mount has also been analyzed and modeled.¹³ A limited amount of stability augmentation is thus available and individual modes can generally be controlled by the choice of variable for feedback such as model position or pitch rate.

In addition to providing stability augmentation, the servo motors may be used to provide excitation forces to the model for response measurements. Excitation is applied as signals to the servo motors in a form suitable for the system identification technique.

The only application of the stability augmentation from the active mount for these tests was for the shuttle orbiter model which was tested at a c.g. position that resulted in an unstable value for $C_{m\dot{\alpha}}$. Feedback proportional to the pitch rate gyro signal stabilized the model. A calculated root locus plot for varying the feedback gain is shown in Fig. 3. With no feedback there are two oscillatory modes. The nearly unstable high-frequency mode is associated with pitching oscillations, and the low-frequency mode is the vertical translation or plunge mode. The addition of pitch rate feedback stabilizes the pitching mode, and with the gain used for the tests [tension increment of 380 N/rad/s (or 1.5 lb/deg/s)] drives the plunge mode to two real roots. It might also be noted that feedback gain can be used as a free parameter to vary for checking trends. Such additional data would enhance the confidence levels of the identified parameters for fixed test conditions and model configuration.

Although the present investigation is limited to low angles of attack or sideslip (as is most aeroelastic testing), tests on the cable mount system can be accomplished by using additional cables to counteract the large lift and trimming forces involved.⁴ The present technique would be applicable, but further consideration of the aerodynamic representation for large angles might be required.

Models and Tests

The models used in this investigation (Fig. 2) are dynamically scaled models that were used for flying characteristics investigations in preparation for flutter tests. They are generally of higher stiffness than scaled values. The tests were performed in the Langley transonic dynamics tunnel. This tunnel has a square 4.88-m (16-ft) slotted test section and is capable of testing at Mach numbers up to 1.2 in air or Freon-12 over a wide range of densities. The models

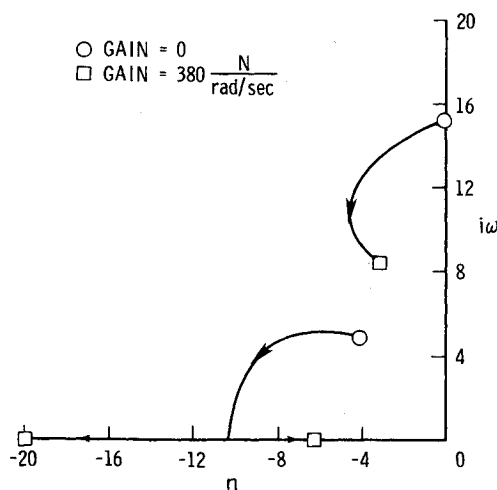


Fig. 3 Effect of pitch rate feedback on longitudinal stability of shuttle model.

were tested at several Mach numbers, dynamic pressures, and with several types and levels of excitation. The tests for the F-14 model reported herein were made in Freon, at a Mach number of 0.865, a dynamic pressure of 3.88 Pa (81 lb_f/ft²), and a rear cable tension of 0.480 kN (100 lb_f). The tests for the shuttle model were also made in Freon at a Mach number of 0.6, a dynamic pressure of 4.79 Pa (100 lb_f/ft²), and a rear cable tension of .970 kN (218 lb_f).

An analytical study was made to determine the type of excitation that would give the best estimates of the parameters. It was found that good results could be obtained by disturbing a trimmed model by turning on an excitation signal containing a combination of all the modal frequencies of the system. The procedure followed in the test was to excite the model with a sinusoidal input and slowly vary the frequency until a peak was found in the response by visual observation of the model and the strip charts. After the modes of the system were found in this manner, the excitation was removed. After the model was steady the excitation containing the modal frequencies was applied and the response measured for data processing.

Instrumentation

A study of the identification process indicates that at least one measured variable is required for each degree of freedom to assure identifiability of the stability derivatives. Additional measurements, however, are desired for redundancy. The study also indicates that direct measurements of angles of attack and sideslip are not essential if cable displacement measurements are made. Thus both model and mount system require instrumentation.

Each model was instrumented with rate gyros for each of the three axes and with vertical and lateral accelerometers. Each of the four cable ends was attached to the model through a strain-gage load cell that permitted dynamic measurement of the cable tension at the model. One of the load cells can be seen in the horizontal forward cable near the fuselage of the F-14 model (Fig. 2a). Although these load cells were large and may have resulted in some aerodynamic interference effects, this arrangement was considered acceptable for this preliminary investigation. With further development, it should be possible to reduce the size of the load cells or have them contained within the model itself.

The displacement and velocity of each cable loop was measured with a potentiometer and a tachometer connected to a pulley shaft. From the pulley position and velocity, cable position and velocity can be calculated, and, with the known cable geometry, the velocity and position of the model can be inferred. Current to the servo motors and the command or excitation voltage were also measured. Instrumentation and control signals from the model were carried to the control room of the wind tunnel by an umbilical running along one of the mount system cables. Test data time histories were recorded on strip chart recorders and were passed through the wind-tunnel data acquisition system and saved on digital tape.

Parameter Estimation Procedure

A block diagram of the elements of the parameter identification procedure is shown in Fig. 4. The SCIPID computer program is a version of a standard maximum likelihood parameter identification program for linear systems developed by Systems Control, Inc. (Vt) and modified to include the influence of the cable system. [The maximum likelihood method is well established in the literature (Refs. 8 and 9, for example) and is not described here.] The SCIPID program requires initial estimates of the coefficients which are calculated by a separate computer program called MAP. Program MAP contains a mathematical model of the cable-mounted aircraft model similar to that of Ref. 12. It takes as input data the test conditions, the mount system geometry, and the initial aerodynamic derivatives, and generates initial values of the coefficients of the linear system containing cable

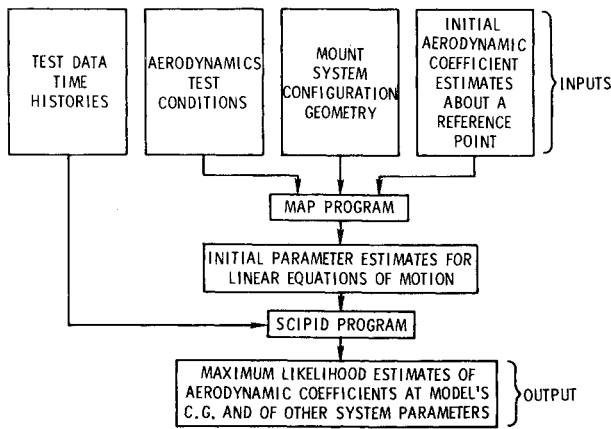


Fig. 4 Block diagram of parameter identification procedure.

effects and aerodynamic effects. It also calculates the eigenvalues and eigenvectors of the system. In addition to the output of MAP, program SCIPID takes the measured time histories of model motions and cable tensions and generates: 1) the maximum likelihood estimates of the derivatives, 2) estimates of the standard deviations of the estimated parameters, 3) instrument biases, 4) state equation initial conditions, and 5) measurement noise covariances. The version of the maximum likelihood method used here allows for measurement noise but does not consider process noise. The recommended procedure is to estimate the aerodynamic derivatives with SCIPID using zero as the initial estimates for the derivatives, in MAP, estimate the biases using the estimated derivatives as fixed parameters, and then estimate both derivatives and biases together. The last step should not result in significant changes in the derivatives for well estimated derivatives.

For two independent estimates of the parameters such as from two different runs, the results can be combined statistically by

$$C^* = (M_1 + M_2)^{-1} (M_1 C_1 + M_2 C_2)$$

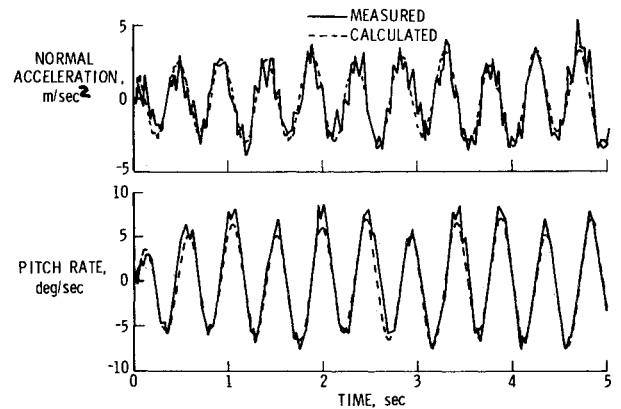
where M_1 , M_2 are the information matrices for runs 1 and 2; C_1 , C_2 are the vectors of parameter estimates for runs 1 and 2; and C^* is the vector of combined parameter estimates. The off-diagonal terms of the M matrices can result in a combined estimate that is not between the two initial estimates.¹¹

The input excitation or forcing function for the identification procedure is considered to be the dynamic tension measured in each cable. The mean values of the tensions form spring effects that are considered analytically in the programs, whereas the incremental or dynamic values of the tensions are applied directly to the model. The line of action of these tensions is calculated from the geometry of the perturbed system based on the pulley rotation measurements and initial geometry. In the past there has been some difficulty in determining derivatives from the mount system using calculated lumped springs and dampings. It is thought that unmodeled nonlinear effects such as pulley rolling friction may have been the source of the difficulty. With direct dynamic measurement of the tensions, such nonlinear effects should be minimized.

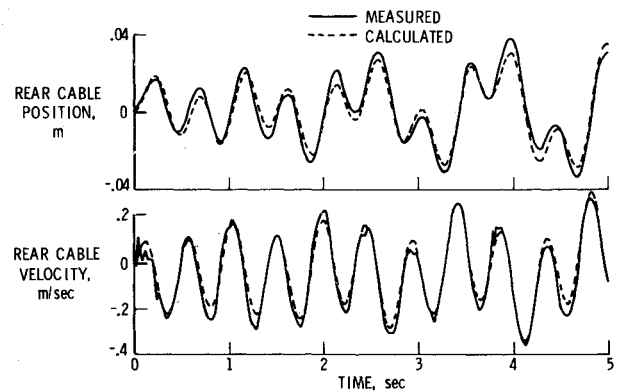
Results and Discussion

Longitudinal Derivatives

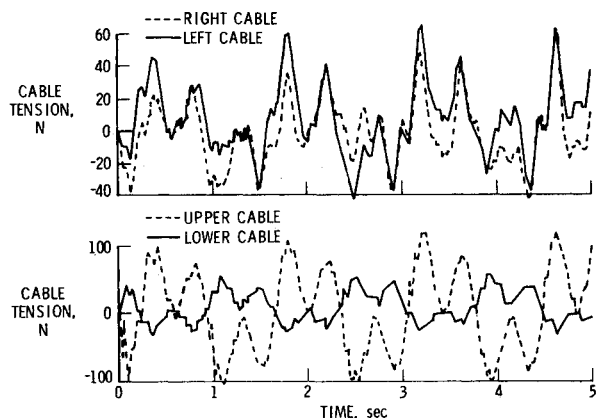
For the test setup and models considered here, three significant aerodynamic derivatives can be estimated: $C_{m_{\dot{\alpha}}}$, $C_{z_{\dot{\alpha}}}$, and $C_{m_q} + C_{m_{\dot{\alpha}}}$. The derivatives are identified from time histories generated by using both a single high-frequency excitation signal and a combined high-and low-frequency excitation signal. Stability derivatives, state initial conditions,



a) Normal acceleration and pitch rate



b) Rear cable position and velocity



c) Cable tensions

Fig. 5 Example longitudinal time histories for the F-14 model showing comparison of measured responses with those calculated using estimated derivatives.

and accelerometer bias are identified. The results along with the initial estimates and standard deviation estimates are shown in Table 1. The initial derivative estimates presented herein were furnished by the manufacturers and represented their estimates for the aircraft based primarily on wind-tunnel tests. The standard deviation estimates, which are based on the Cramer-Rao bound, serve as a lower bound to the standard deviations. They serve as a basis of comparison between estimates rather than absolute indicators.

The results for the F-14 model (Table 1) are in good agreement except for the quantity $C_{m_q} + C_{m_{\dot{\alpha}}}$. Measured time histories are compared in Figs. 5a and 5b with those calculated using the extracted derivatives and measured input excitation. Time histories of the measured tension increments are presented in Fig. 5c. The case shown is for two frequencies of excitation, and a good comparison is obtained. The reason

Table 1 Estimates for F-14 and shuttle longitudinal coefficients

		Estimates (standard deviations)		
		Initial estimates	High-frequency excitation	Low-frequency excitation
F-14	$C_{Z\alpha}$	- 5.88	- 5.63(0.019)	- 5.91 (0.013)
	$C_{m\dot{q}} + C_{m\dot{\alpha}}$	-24.3	-13.2 (0.11)	-14.8 (0.20)
	$C_{m\alpha}$	- 2.87	- 2.89 (0.0028)	- 2.92 (0.0062)
Shuttle orbiter	$C_{Z\alpha}$	- 2.51	- 3.86 (0.105)	- 2.82 (0.054)
	$C_{m\dot{q}} + C_{m\dot{\alpha}}$	- 2.40	- 3.75 (0.099)	- 2.68 (0.045)
	$C_{m\alpha}$	+ 0.164	+ 0.158 (0.00084)	+ 0.166 (0.00050)

Table 2 Estimates for F-14 lateral coefficients

		Estimates (standard deviations)		
		Initial estimates	High-frequency excitation	Low- and high-frequency excitation
$C_{Y\beta}$	-1.06	-0.424 (0.045)	-0.827 (0.020)	-0.972 (0.014)
C_{Yp}	-0.034	1.58 (0.16)	-0.355 (0.080)	-0.611 (0.053)
C_{Yr}	0.378	1.58 (0.12)	3.79 (0.13)	3.46 (0.067)
$C_{l\beta}$	-0.111	-0.020 (0.0020)	-0.028 (0.0006)	-0.028 (0.0004)
C_{lp}	-0.186	-0.111 (0.0072)	-0.174 (0.0021)	-0.147 (0.0016)
C_{lr}	0.083	0.522 (0.0057)	0.582 (0.0068)	0.547 (0.0031)
$C_{n\beta}$	0.151	0.092 (0.0037)	0.086 (0.0027)	0.097 (0.00019)
C_{np}	0.024	-0.151 (0.013)	-0.189 (0.011)	-0.136 (0.007)
C_{nr}	-0.123	-0.574 (0.0087)	-0.473 (0.012)	-0.562 (0.0059)

Table 3 Estimates for shuttle lateral coefficients

		Estimates (standard deviations)		
		Initial estimates	2-frequency excitation	3-frequency excitation
$C_{Y\beta}$	-0.920	-1.204 (0.0090)	-0.858 (0.0047)	-0.935 (.0039)
$C_{l\beta}$	-0.0458	-0.0395 (0.0011)	-0.0322 (0.0012)	-0.0323 (0.0008)
C_{lp}	-0.288	-0.314 (0.0031)	-0.305 (0.0041)	-0.306 (0.0024)
C_{lr}	0.127	0.0965 (0.0095)	0.122 (0.012)	0.103 (0.0073)
$C_{n\beta}$	0.0436	-0.0128 (0.00050)	-0.0288 (0.00067)	-0.0221 (0.00021)
C_{np}	0.194	-0.0075 (0.0040)	-0.0080 (0.0077)	0.0108 (0.0023)
C_{nr}	-0.231	-0.182 (0.0023)	-0.180 (0.0031)	-0.167 (0.0012)

for the discrepancy in $C_{m\dot{q}} + C_{m\dot{\alpha}}$ is unknown. Possible reasons are that the initial estimate of $C_{m\dot{q}} + C_{m\dot{\alpha}}$, which if for the aircraft, may not be a reliable estimate for the model tested, or there may be a system modeling error for this case. The combined estimates were used to predict the time histories for another point that was excited at the plunge frequency only. Fair correlation was obtained (not shown). Identification of the coefficients from the latter point gave a better fit to the time histories, about the same values for $C_{m\dot{q}}$ and $C_{Z\alpha}$, but a larger negative value of $C_{m\dot{q}} + C_{m\dot{\alpha}}$ that had a larger standard deviation. It appears that for the F-14 the combined results for $C_{Z\alpha}$ and $C_{m\alpha}$ are extracted with good reliability, but that $C_{m\dot{q}} + C_{m\dot{\alpha}}$ is less well determined.

Corresponding results for the shuttle orbiter (Table 1) are also in reasonable agreement with initial estimates but with more variability than for the F-14. As previously mentioned the value of $C_{m\dot{q}}$ for this model was positive (unstable). As a result, even with the feedback system operating, the force required to excite the model was quite small. The resulting tension increments were small and noisy. In addition, the time histories contained a small-amplitude pitching oscillation. These factors apparently prevented a solution from being obtained using the identification procedure recommended in the previous section. The results of Table 1 were, therefore, obtained by simultaneous identification of derivatives, state initial conditions, and accelerometer bias using the initial values as starters. This procedure increases the risk of finding a local minimum of the cost function by the identification algorithm, as the results depend on the initial estimates.

Comparisons of the measured and calculated time histories were generally good, although in some instances the comparisons were only fair.

One item that caused some concern in the initial stage of this investigation of the shuttle data was that two peak values were found by exciting the model sinusoidally, whereas Fig. 3 indicates that there should only be one oscillatory mode. However, the frequency response functions for this case, calculated using the program of Ref. 13 (and initial derivative estimates) are presented in Fig. 6. A second peak for the pitch rate gyro occurs near the value determined experimentally. This peak was considered a mode during the test, but rather

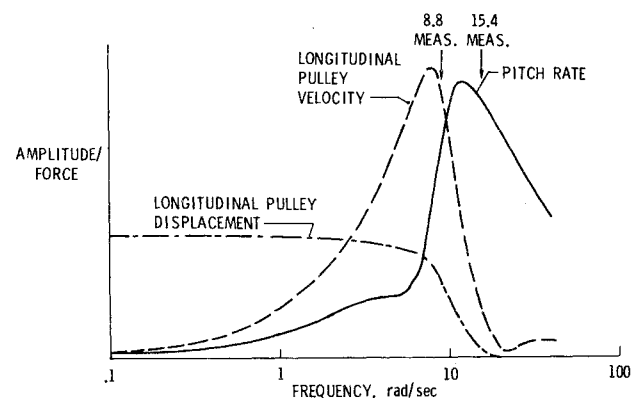


Fig. 6 Frequency response functions for shuttle orbiter model.

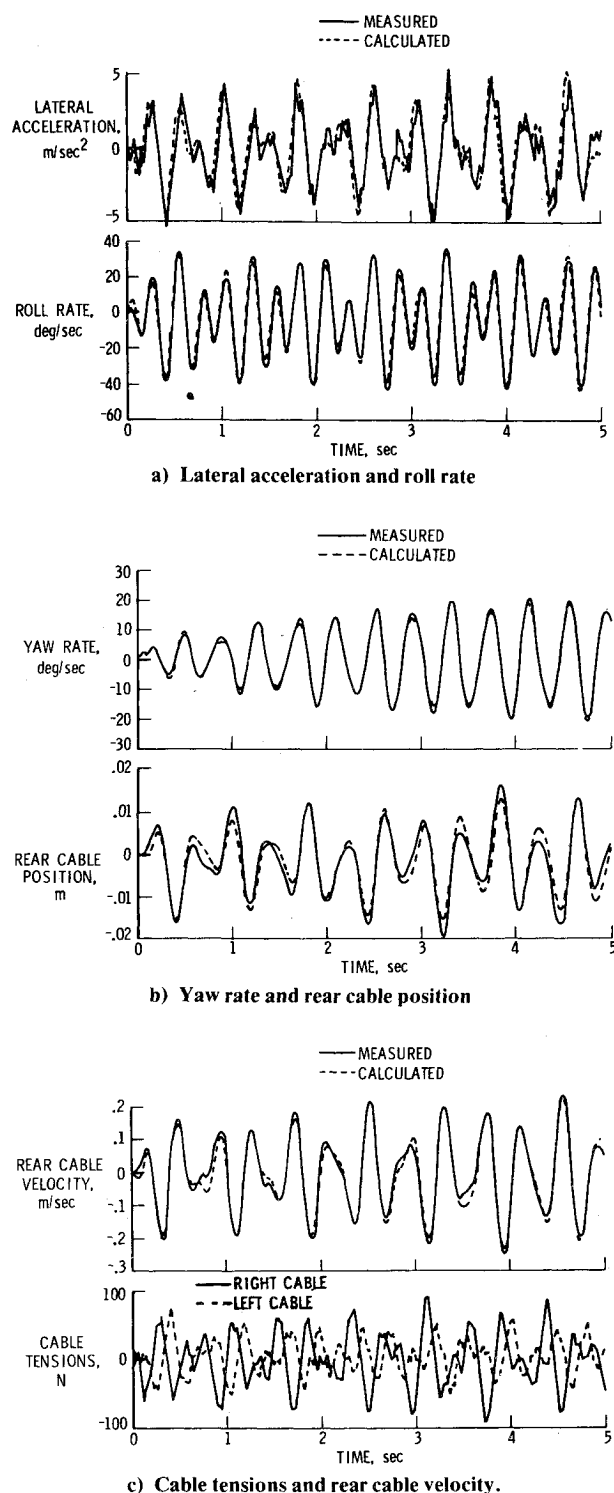


Fig. 7 Example lateral time histories for shuttle orbiter model showing comparison of measured responses with those calculated using estimated derivatives.

than corresponding to a mode, it was evidently a result of the manner in which the model was forced. Overall it would appear that the shuttle longitudinal case is a severe test for the technique, and although reasonable values of the derivatives are estimated, the confidence placed in the estimates may be low.

Lateral Derivatives

The lateral results for the F-14 are presented in Table 2 for the same test conditions as for the longitudinal cases. Reasonably good correspondence with initial estimates are

shown for the more significant derivatives ($C_{Y\beta}$, $C_{l\beta}$, C_{lp} , $C_{n\beta}$, and C_{nr}) with generally larger deviations in those of lesser importance (for the low angles of attack considered here, β effects are assumed added to the r derivatives). The derivatives C_{nr} and $C_{l\beta}$ are rather different from initial estimates, however, although the identified results are relatively consistent. Good comparisons of the measured and calculated time histories were obtained. For these cases the pulley potentiometer was defective and therefore measurements of lateral model displacement were deleted. Derivatives estimates were still obtained as this measurement would have been a redundant data channel.

Lateral results for the shuttle orbiter are presented in Table 3. For this case the derivatives C_{Yp} and C_{Yr} were fixed at their initial values. In Fig. 7 the measured time histories of a case of two-frequency excitation are compared with the calculated time histories using the extracted derivatives. The measured tension increment time histories that are inputs are shown in Fig. 7c. The results for the lateral derivatives (Table 3) indicate good correspondence with initial values except for C_{np} , which is of lesser importance, and for $C_{n\beta}$. In each case the value extracted for $C_{n\beta}$ is of opposite sign (statically unstable) although small. The estimate of $C_{n\beta}$ may be hampered because the cable-mount yaw spring was large in comparison with the aerodynamic spring in this case.

Although the comparison of the extracted derivatives with initial estimates and the comparison of calculated time histories with measured time histories (including other points) are not absolute standards, there is an overall indication that reasonable results can be obtained with this system. This conclusion is based on the results from a few points for two models and further experience and evaluation are desirable. It also appears that only the derivatives of primary importance can be well determined by this technique (as is the case with most indirect methods). It does not appear practical to resolve secondary effects such as separating α and q contributions to longitudinal derivatives.

Concluding Remarks

System identification techniques in common use for extracting stability derivatives from flight test data have been applied to data obtained from two dynamic models flown in a wind tunnel on a cable-mount system. The results for both lateral and longitudinal derivatives for each model generally appear to be reasonable when compared with derivatives obtained from other sources and when used to predict other data points. Further application of this new technique should provide useful information on the stability derivatives of flexible aircraft.

References

- Reed, W. H. III and Abbott, F. T. Jr., "A New Free-Flight Mount System for High Speed Wind-Tunnel Flutter Models," *Proceedings of the Symposium on Aeroelastic Dynamic Modeling Technology*, U.S. Air Force Systems Command, RTD-TDR-63-4197, Pt. 1, 1964.
- Gilman, J. Jr. and Bennett, R. M., "A Wind-Tunnel Technique for Measuring Frequency-Response Functions for Gust Load Analysis," *Journal of Aircraft*, Vol. 3, Nov.-Dec. 1965, pp. 535-540.
- Abel, I., "Evaluation of a Technique for Determining Airplane Aileron Effectiveness and Roll Rate by Using an Aeroelastically Scaled Model," NASA TN-D-5538, Nov. 1969.
- Rainey, A. G. and Abel, I., "Wind-Tunnel Techniques for the Study of Aeroelastic Effects on Aircraft Stability, Control, and Loads," *AGARD Flight Mechanics Panel*, Marseille, France, AGARD CP-46, March 1970.
- Rodden, W. P., "Dihedral Effect of a Flexible Wing," *Journal of Aircraft*, Vol. 2, Sept.-Oct. 1965, pp. 368-373.
- Rodden, W. P., "Extension of an Aeroelastic Parameter for Estimation of the Effects of Flexibility on the Lateral Stability and Control of Aircraft," *Journal of the Aeronautical Sciences*, Vol. 24, Aug. 1957, pp. 624-625.
- Illiff, K. W. and Maine, R. E., "Practical Aspects of Using a Maximum Likelihood Estimation Method to Extract Stability and

Control Derivatives from Flight Data," NASA TN D-8209, April 1976.

⁸"Method for Aircraft State and Parameter Identification," *Specialist Meeting of the Flight Mechanics Panel of AGARD*, Hampton, Va., AGARD-CP-172, May 1975.

⁹"Parameter Estimation Techniques and Applications in Aircraft Flight Testing," *Symposium at Flight Research Center*, Edwards, Calif., April 24-25, 1973, NASA TN D-7647, April 1974.

¹⁰Mehra, R. K., Stepner, D. E., and Tyler, J. S., "Maximum Likelihood Identification of Aircraft Stability and Control

Derivatives," *Journal of Aircraft*, Vol. 11, Feb. 1974, pp. 81-88.

¹¹Mohr, R. L. and Hall, W. E. Jr., "Identification of Stability Derivatives from Wind-Tunnel Tests of Cable-Mounted Aeroelastic Models," NASA CR-145123, 1977.

¹²Barbero, P. and Chin, J., "User's Guide for a Computer Program to Analyze the LRC 16' Transonic Dynamics Tunnel Cable-Mount System," NASA CR-132313, 1973.

¹³Chin, J. and Barbero, P., "User's Guide for a Revised Computer Program to Analyze the LRC 16' Transonic Dynamics Tunnel Active Cable-Mount System," NASA CR-132692, 1975.

From the AIAA Progress in Astronautics and Aeronautics Series . . .

TURBULENT COMBUSTION—v. 58

Edited by Lawrence A. Kennedy, State University of New York at Buffalo

Practical combustion systems are almost all based on turbulent combustion, as distinct from the more elementary processes (more academically appealing) of laminar or even stationary combustion. A practical combustor, whether employed in a power generating plant, in an automobile engine, in an aircraft jet engine, or whatever, requires a large and fast mass flow or throughput in order to meet useful specifications. The impetus for the study of turbulent combustion is therefore strong.

In spite of this, our understanding of turbulent combustion processes, that is, more specifically the interplay of fast oxidative chemical reactions, strong transport fluxes of heat and mass, and intense fluid-mechanical turbulence, is still incomplete. In the last few years, two strong forces have emerged that now compel research scientists to attack the subject of turbulent combustion anew. One is the development of novel instrumental techniques that permit rather precise nonintrusive measurement of reactant concentrations, turbulent velocity fluctuations, temperatures, etc., generally by optical means using laser beams. The other is the compelling demand to solve hitherto bypassed problems such as identifying the mechanisms responsible for the production of the minor compounds labeled pollutants and discovering ways to reduce such emissions.

This new climate of research in turbulent combustion and the availability of new results led to the Symposium from which this book is derived. Anyone interested in the modern science of combustion will find this book a rewarding source of information.

485 pp., 6 × 9, illus. \$20.00 Mem. \$35.00 List

TO ORDER WRITE: Publications Dept., AIAA, 1290 Avenue of the Americas, New York, N. Y. 10019